Study of the influence of NH$_3$ flow rates on the structure and photoluminescence of silicon-nitride films with silicon nanoparticles

A. López-Suárez [a,*], J. Fandiño [b], B.M. Monroy [c], G. Santana [c], J.C. Alonso [c]

[a] *Instituto de Física, Universidad Nacional Autónoma de México, Ap. Postal 20-364, México, DF 01000, México*
[b] *Universidad Autónoma de la Ciudad de México, Av. Providencia s/n, Col. San Lorenzo Tezonco, Delegación Iztapalapa, DF, México*
[c] *Instituto de Investigaciones en Materiales, Universidad Nacional Autónoma de México. A.P. 70-360, Coyoacán 04510, DF, México*

A R T I C L E   I N F O

A B S T R A C T

Silicon-nitride films with silicon nanoparticles have been prepared at 300 °C by remote plasma-enhanced chemical vapor deposition using mixtures of H$_2$, Ar and SiH$_2$Cl$_2$ and various NH$_3$ flow rates. The films were characterized by means of Rutherford backscattering spectrometry, Fourier-transform infrared spectroscopy, single wavelength ellipsometry, high-resolution transmission electronic microscopy, atomic force microscopy and photoluminescence measurements. It was found a chemical stability as well as an increase in the photoluminescence signal for those films with the greatest amount of NH$_3$. The increase in the photoluminescence signal is due to a quantum confinement effect produced by the nanoparticles, which were formed during the film's preparation process.

1. Introduction

For a long time, bulk silicon has been considered a very important material for the microelectronic industry. However, it has not been used for optoelectronic applications because it has a limited efficiency as a light emitter in the visible range due to its indirect band gap of 1.1 eV. In recent years, a number of studies [1,2] have shown that room temperature light emission from silicon is possible when it is in the form of low dimensional size, such as porous silicon and silicon nanostructures. The visible photoluminescence (PL) due to silicon nanostructures can be the result of the quantum confinement effect, which predicts that the energies of the valence band and the conduction band edges are shifted relative to the bands of the bulk silicon, producing an increase in the energy gap.

Experimental techniques have been attempted to obtain Si nanostructures, such as chemical vapor deposition [3,4], Si ion implantation into SiO$_2$ [5], cluster ion-beam deposition [6], sputtering [7], laser ablation [8] and thermal vaporization [9,10]. In this study, we use the remote plasma-enhanced chemical vapor deposition (RPECVD) to form the silicon-nitride matrix where the Si nanostructures are formed. The main advantage of RPECVD technique over the commonly used plasma-enhanced chemical vapor deposition (PECVD) technique is that there is more control on the chemical reactions during the growing of the thin film, which means that it can be gotten a better matrix material. Although silicon oxide thin films has been widely used as the matrix for embedding photoluminescent silicon nanoparticles, there is much interest in using silicon-nitride films because its lower band gap compared with silicon dioxide that facilitates charge carrier injection for the fabrication of electroluminescent devices. This was the principal motivation to investigate the PL properties of the silicon-nitride films prepared by high density-inductively couple RPECVD from NH$_3$/H$_2$/SiCl$_2$H$_2$/Ar mixtures. We emphasized this study on changing the NH$_3$ flow rate, so we could be able to study the differences in the PL signal as the ammonia gas is increased; due to the NH$_3$ hydrogen atoms passivate the non-radiative defects enhancing the PL in silicon.

* Corresponding author. Tel.: +52 55 56 22 50 02; fax: +52 55 56 22 50 09.
E-mail addresses: chipi72@gmail.com, chipi@fisica.unam.mx (A. López-Suárez).

2. Experiment

The silicon-nitride films were prepared using a RPECVD system manufactured by MV-Systems Inc (CO, USA). The system characteristics have been reported in Ref. [11]. The films were grown on $(1\,0\,0)$ n-type silicon crystalline substrates, using a working pressure of 300 mTorr, a substrate temperature of 300 °C and a radio frequency power of 150 W. The flow rates of H_2, Ar and SiH_2Cl_2 were 20, 150 and 5 sccm, respectively. The flow rate of NH_3 was varied from 0 to 50 sccm. Before the deposition, the substrates were cleaned for 5 min using a "p-etch solution," which consists of 300:15:10 parts of H_2O:HNO_3:HF. During the deposition, Ar and NH_3 gases were fed from the top of the chamber where the plasma is formed; meanwhile, the H_2 and SiH_2Cl_2 gases were fed from the side and underneath the plasma by means of a dispersal ring located over the substrate holder.

During the whole work, samples will be denoted by Si-X, where Si means that the film has been grown on a silicon substrate and X corresponds to the NH_3 flow rate that was used to prepare each sample. For instance, Si-25 denotes that the sample was prepared with a NH_3 flow rate equal to 25 sccm.

Rutherford backscattering spectrometry (RBS) was used to determine the elemental composition of the film. A collimated 3.045 MeV α-particle beam of 2 mm diameter, with a mean 50 nA ion current and a beam charge of 30 μC was used to obtain the atomic concentration of Si, N, Cl and O in the samples. These experiments were performed using the 3 MV Tandem accelerator (NEC 9SDH-2 Pelletron) facility at the Instituto de Física of the Universidad Nacional Autónoma de México (UNAM). Projectiles that scattered at 168° were detected with an OXFORD 50-11 surface barrier detector. The simulation and analysis of the RBS spectra was done with the SIMNRA code [12], which allows the non-Rutherford backscattering spectra to be simulated. We took advantage of the elastic scattering resonance $^{16}O(\alpha,\alpha)^{16}O$ at

3.045 MeV, that is 25 times larger than its corresponding Rutherford cross section, in order to obtain high sensitivity in the oxygen measurement.

Chemical bond analysis was determined ex situ using a Fourier transform infrared (FTIR) spectrophotometer (Nicolet 210), operated in the range of 400–4000 cm^{-1}, with an 8 cm^{-1} resolution. For each sample, a reference spectrum of a silicon substrate was subtracted from the experimental spectra. The samples were characterized by the high-resolution transmission electronic microscopy (HRTEM) at the Instituto de Fisica of the UNAM. HRTEM was performed using a JEOL JEM-2010F FasTEM microscope operating at 200 kV and equipped with a GATAN digital micrograph system for image acquisition (version 3.7.0). Atomic force microscopy images were obtained from a JEOL JSPM-4210/TM-4210BU in the tapping mode. PL experiments were performed at room temperature in a conventional PL system at the Instituto Politécnico Nacional (IPN). The PL system's characteristics are described in Ref. [13].

3. Results and discussion

The chemical bonds present in the films were determined by FTIR transmission analysis. The FTIR spectra of the silicon-nitride films deposited under different NH_3 flow rates are observed in Figs. 1 and 2. The FTIR transmission spectrum shown in Fig. 1 for the sample prepared without NH_3, is typical of a hydrogenated amorphous silicon film (a-Si:H), since it only shows two small bands at 638 and 2100 cm^{-1}, associated to wagging and stretching Si–H bonds, respectively [14]. The other small absorption band located at 550 cm^{-1} corresponds to Si–Cl_2 bonds [15]. The rest of FTIR spectra in Fig. 1 show absorption bands located around 3150, 3037, 2819 and 1415 cm^{-1}, which correspond to Si–NH_2 vibrations [16]. The absorption bands located at 1062 and 492 cm^{-1} are
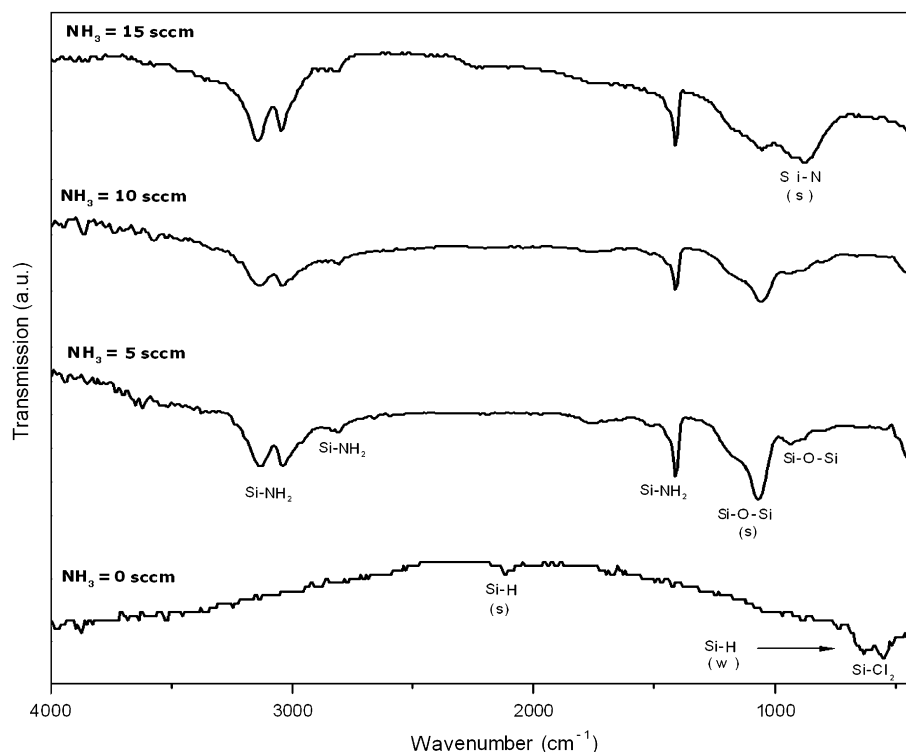

Fig. 1. FTIR transmission spectrum of samples deposited with NH_3 flow rates lower than 15 sccm.
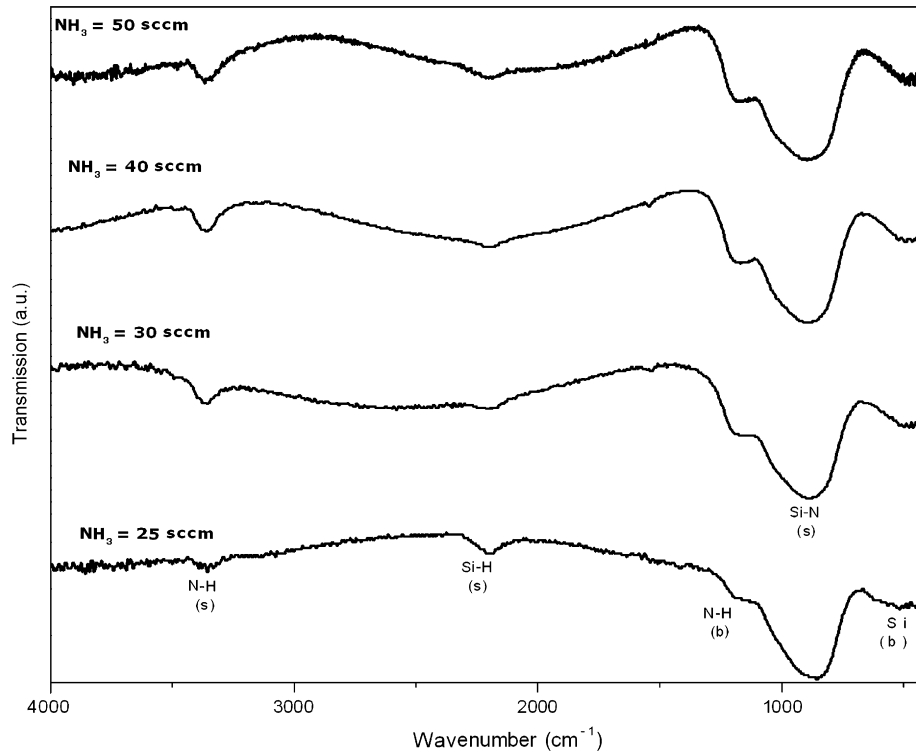
Fig. 2. FTIR transmission spectrum of samples deposited with NH_3 flow rates larger than 15 sccm.

related to stretching and rocking vibrations of Si–O–Si bonds, respectively [15], meanwhile the one located at $929\,cm^{-1}$ corresponds to Si–OH bonds [17]. Since there is no oxygen present in the chamber during films deposition, the appearance of these bands is unexpected and obeys to a post-deposition films transformation. We believe that the relative low content of hydrogen present in the chamber during the growing process allows a great amount of Cl to incorporate in the film network, with at least two important consequences: films network become more open (since Cl forms terminal bonds) and also important amounts of Cl are forming chemical unstable bonds in as grown films, so when the films are uploaded from the deposition system and expose to the atmosphere, the oxygen and water vapor present in it could diffuse into the films, and complex chemical reactions take place leading to the formation of non-stoichiometric silicon oxide with a reduced amount of chlorine. The excess of Cl is removed by means of solids and possibly gaseous reaction byproducts such as NH_4Cl and HCl, respectively. Evidence of the former has been found at the films surface after an hour of ambient exposure, forming a deposit with an off-white aspect that was easily removed by immersion in water. The films that undergo such uncontrollable post-deposition transformations will be further denoted as class I films.

Fig. 2 shows the spectra of the samples deposited with NH_3 flow rates larger than 15 sccm. The main absorption band located at $863\,cm^{-1}$ observed in these spectra is due to stretching vibration of Si–N bonds [11]. The bands located around 3356 and $1155\,cm^{-1}$ correspond to stretching and bending vibrations of N–H bonds, respectively; meanwhile, that at $2205\,cm^{-1}$ is related to stretching modes of Si–H bonds. Finally, the small band around $485\,cm^{-1}$, can be associated to Si atom breathing vibrations [18]. It is not clear the presence of Si–Cl bonds in the films, whose corresponding bands should appear between 500 and $650\,cm^{-1}$ [15]. It is observed from the FTIR spectra that the bending and the

stretching N–H bands increase in size with the ammonia concentration, what is in perfect agreement with the experiment.

Qualitative differences arise by comparing the spectra in Figs. 1 and 2. In contrast with the behavior observed in the spectra depicted in Fig. 1, the spectra in Fig. 2 show no clear evidence of oxygen-related bonds; in fact, if small amounts of Si–O–Si bonds exists, their main vibration absorption band (located around $1070\,cm^{-1}$) must be veiled by the broad band corresponding to Si–N stretching mode. Also, the broad multi-peak bands associated to $SiNH_2$ vibrations in Fig. 1 are substituted by a small single-peak band related to N–H bonds in Fig. 2. This abrupt change in the films bonding structure as a function of ammonia flow rate could be understood, as mentioned earlier, in terms of the hydrogen role as chlorine gathering agent during film formation. When there is enough hydrogen content in the chamber, silicon-nitride films are able to grow with low content of chlorine in their network, making them chemically more stable than those previously denoted as class I films, so no chemical reaction takes place when these films make contact with the atmosphere. For this reason, the films deposited with ammonia flow rates larger than 15 sccm will be further named as class II films.

The elemental concentrations of the components of the films were obtained from RBS measurements using a 3.045 [4]He beam. RBS is a very accurate, sensitive and non-destructive technique used to measure the elemental composition of a sample. During a RBS study, a beam of collimated and monoenergetic particles generated by an accelerator collide with the sample. Particles are scattered out of the target and reach a silicon surface barrier detector where they are analyzed. The analog signals that leave this system are processed by a multi-channel analyzer to form the RBS spectra. In this method, the element to be analyzed is identified by the energy and type of the emitted particles coming from a specific reaction between the incident ion and the given
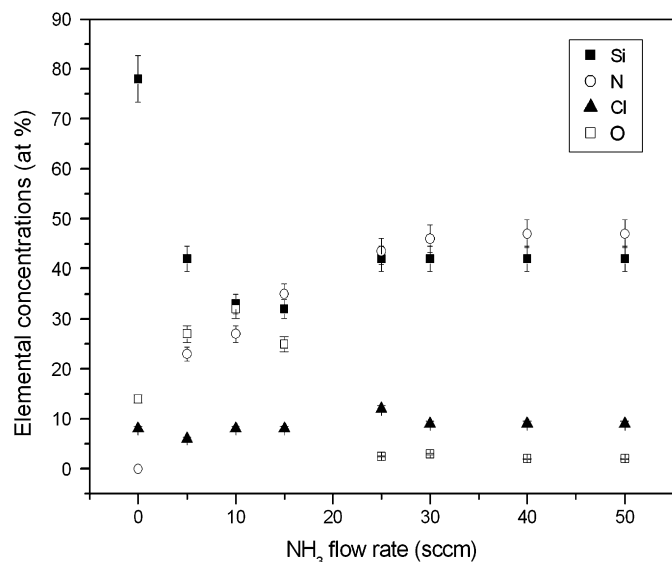
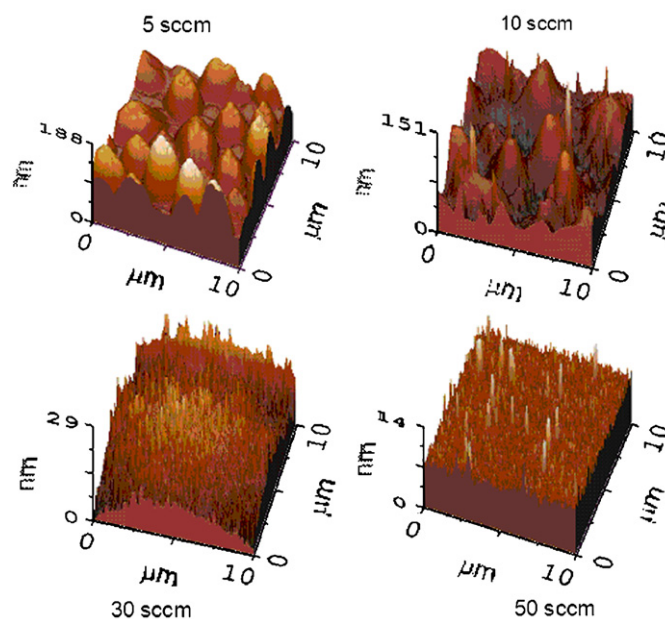**Fig. 3.** RBS results of the film composition as a function of NH$_3$ flow rates.

Fig. 4. AFM images of silicon-nitride films deposited at 5, 10, 30 and 50 NH$_3$ flow rates.

Fig. 5. Root mean square roughness (RMS) of film surface as a function of ammonia flow rates.

target element. The atomic percentage concentrations of the detected elements as a function of the NH$_3$ flow rates are plotted in Fig. 3, where the two previously defined groups of samples are easily seen. The separation of both zones exhibits abrupt changes in the elemental composition of the films. In agreement with FTIR measurements (Fig. 1), the films that belong to class I contain higher concentration of oxygen in their networks, making their chemical composition typical to that of silicon oxynitrides (instead of silicon nitride or silicon dioxide) with the exception of the sample grown without ammonia, which contains almost 80% of silicon; this means that this sample behaves as an amorphous silicon film. On the other hand, the RBS results show that the films that belong to class II have atomic composition near to that of stoichiometric silicon nitrides (Si$_3$N$_4$), what make them to be chemically stable.

The N concentration, which was introduced into the system as the main variable in the form of NH$_3$, increases in the films until it reaches 46 at% at the Si-30 sample. From this point until the Si-50 sample, a saturation behavior for N is observed. In the case of O, the samples grown with lower NH$_3$ flow rates (class I films) show a relatively high concentration of this element. This behavior can be seen as a maximum increment of 32 at% in the oxygen concentration for the Si-10 sample. For class II films, the oxygen concentration shows an abrupt decrement, with a detecting signal lower than 3 at%. In order to obtain this small oxygen signal, that was not detected during the FTIR studies (Fig. 2), we had to take advantage of the versatility of the RBS technique that allows increasing the oxygen signal by using one of its resonance energies (3.045 MeV). The RBS oxygen results support the previous statement that oxygen enters into the class I films networks as a consequence of post-deposition chemical reactions.

In order to show the typical behavior of films surface morphologies, two samples of each class were chosen and their respective three-dimensional AFM images were depicted in Fig. 4. In general, class I films have rough surfaces, with round peak and valleys of relatively wide area, and heights in the order of hundred of nanometers. When the ammonia flow rate increases in the chamber, the resulting films surface has smaller features up to the Si-50 sample, which shows a surface morphology typical of PECVD amorphous silicon-nitride films. The results can be
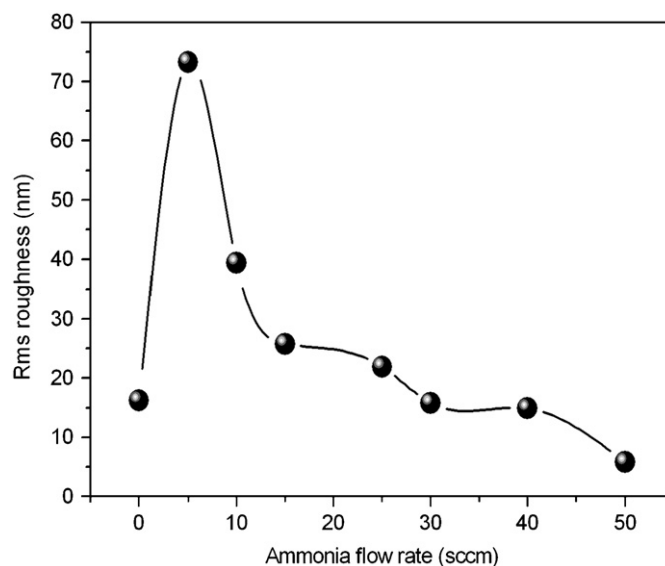
observed in Fig. 5, where the root mean-squared roughness values were calculated from de AFM images.

These results could be possibly understood in terms of the differences in the chemical composition of the plasma during films growth. At low values of the NH$_3$ flow rates, there is no enough hydrogen in the chamber to remove appreciable amounts of Cl from the SiH$_2$Cl$_2$-related species. This excess of chlorine in the form of terminal bonds could be acting as a diffusion barrier for the growing species, lowering their diffusion coefficient and creating roughness surfaces. As the ammonia flow rate increases, more hydrogen is available in order to remove chlorine from the chemical active species leading less chlorine at the growing surface. This fact contributes to enhance the superficial diffusion

coefficients in such a way that smoother films surface are obtained as the ammonia flow rate increases.

Along the present study the silicon-nitride films have formed two well-defined groups according to their ammonia concentration, which can be confirmed with the PL measurements. In the as-prepared samples, the PL intensity is low, almost null, for class I films, while for class II samples the PL spectra show intense and well-defined peaks that cover the energy axis from 1.5 to 3.25 eV. The Si-25 sample shows a unique peak with its maximum located at 2.06 eV. This peak is also observed in the other three PL spectra, but it appears shifted to the right. The PL spectrum of the Si-30 sample shows the formation of four peaks in the range of 2.16–2.99 eV; while samples Si-40 and Si-50 show five peaks each one, as can be seen in Table 1 and Fig. 6. The intensity of the PL peaks increases according to the ammonia concentration.

Some authors suggest that the PL origin in these films is produced by a quantum confinement effect in the silicon nanoparticles embedded in nitride matrix [3,19–21]. Some others [1,2,22] also suggest that the presence of different PL peaks means that the sample is formed by nanoparticles of different size that produce this confinement effect. In order to confirm this fact, we will focus on the HRTEM studies of the two samples (Si-50 and Si-10) that show the biggest contrast in their PL signals. An EDX

measure was performed to the Si-50 sample in order to verify the composition of the nanoparticles that were formed during the growing process. The results show the following elemental concentrations: 95% Si, 3% O and 2% Cu. The Cu signal comes from the Cu grating where the film was supported. Fig. 7a shows the HRTEM micrograph of silicon nanoparticles embedded in a silicon-nitride film in the case of the Si-50 sample. The silicon nanoparticles appear as dark rounded spots, while the silicon substrate appears as a lighter region surrounding the nanoparticles. The average size of the silicon nanocrystals is 6.9 nm. Crystallographic planes of a silicon nanoparticle as well as the orientation of the crystalline planes given by the Fourier transform of the previous nanoparticle image are shown in Fig. 7b. The use of chlorinated silicon precursors during the study could be the responsible of the crystallinity of the as-grown silicon nanoparticles, as was shown by Shirai et al. [23] and Monroy et al. [24].

Fig. 8 shows the HRTEM micrograph of the sample with NH_3 flow rate equal to 10 sccm. In this case, the particles founded are rounded and their average size is 26.1 nm. We think that the difference in PL between both samples is due to the size and density of the nanoparticles and not because the presence of the particles indeed. We assume that the PL is due to a quantum confinement effect produced by the size of the particle as well as the passivation of the surface produced by the hydrogen and nitrogen derived from the NH_3. The multiple peaks observed in the PL spectra are originated by the size distribution of nanoparticles inside the matrix.

4. Conclusions

Silicon-nitride films have been prepared at low temperature (300 °C) by RPECVD using mixtures of H_2, Ar and SiH_2Cl_2 and NH_3. The variation of the NH_3 flow rates on the structural and optical properties of the films has been examined. It was found that the films can be divided in two classes depending on the NH_3 concentration. Those films in the range of 25–50 sccm NH_3 flow rates exhibit a chemical stability as well as an increase in the PL
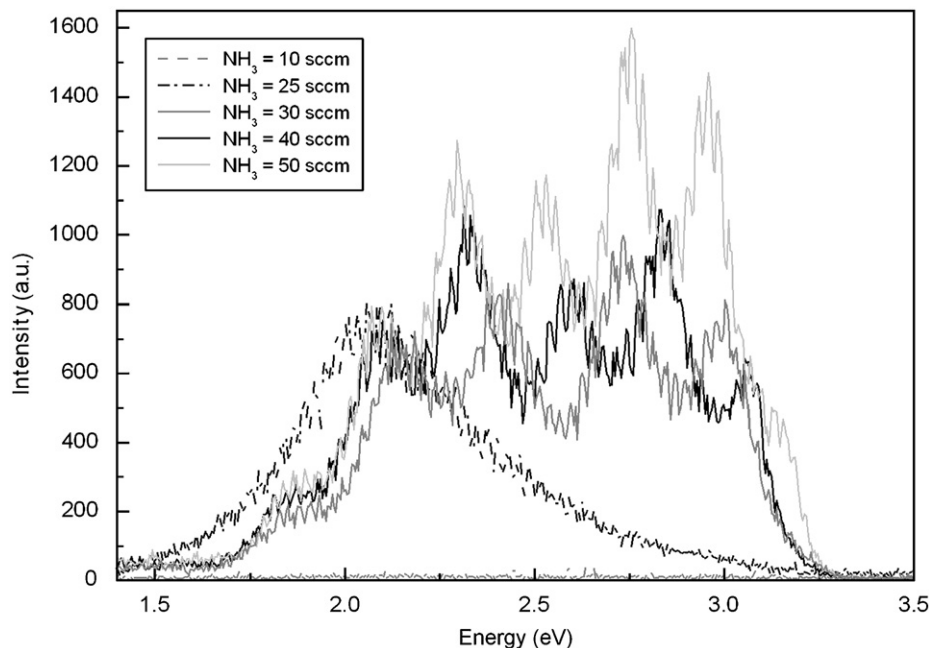
Table 1
Position of the different PL peaks in the silicon-nitride films

Sample	Position of the peaks (eV)
Si-5	No observed
Si-10	No observed
Si-15	No observed
Si-25	2.06
Si-30	2.16, 2.41, 2.73, 2.99
Si-40	2.10, 2.33, 2.60, 2.84, 3.06
Si-50	2.10, 2.30, 2.52, 2.75, 2.96

Fig. 6. PL spectra of films that show the greater photoluminescence signal. Several peaks can be observed in those samples with the greater NH_3 flow rates.
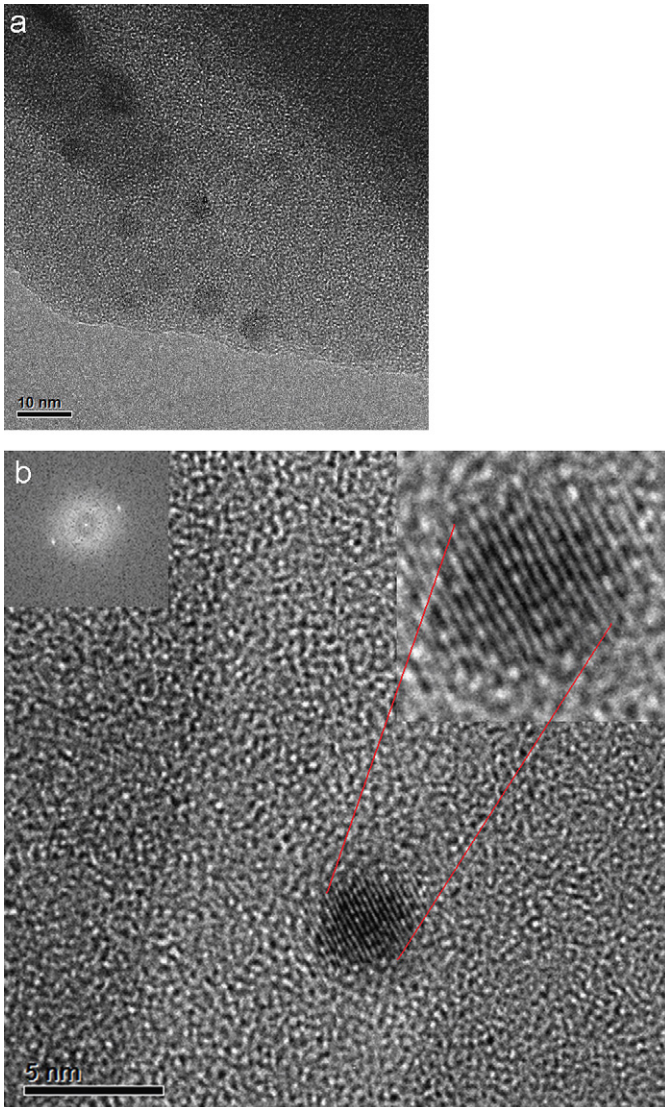
Fig. 7. (a) HRTEM micrographs of Si-50 sample. Silicon nanoparticles of 6.46 mean size embedded in a silicon-nitride film are shown. (b) Crystallographic planes and the FFT of one of the nanoparticles presented in the film.
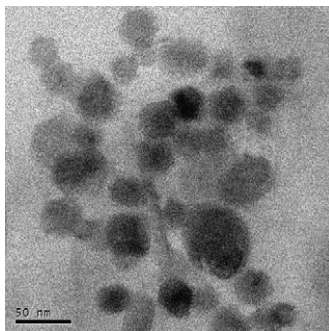

Fig. 8. HRTEM micrograph of Si-10 sample. A distribution in size of nanoparticles is shown. The mean size of these nanoparticles is 26.58 nm.

signal. It was also found that the PL signal is produced by the quantum confinement due to the nanoparticles that were create inside the material during the growing process and is not an effect due to the porous silicon indeed.

References

[1] Tae-Wook Kim, et al., Appl. Phys. Lett. 88 (2006) 123102.
[2] Nae-Man Park, et al., Phys. Rev. Lett. 86 (2001) 1355.
[3] Y.Q. Wang, et al., Appl. Phys. Lett. 83 (2003) 3474.
[4] N.M. Park, et al., Appl. Phys. Lett. 78 (2001) 2575.
[5] T.S. Iwayama, T. Miyasato, Jpn. J. Appl. Phys. 27 (1998) L2207.
[6] M. Ehbrechet, et al., Appl. Phys. Lett. 79 (2001) 4028.
[7] P.M. Fauchet, et al., Opt. Mater. 27 (2005) 745.
[8] L. Patrone, et al., J. Appl. Phys. 87 (2000) 3829.
[9] L.N. Dinh, et al., Phys. Rev. B 54 (7) (1996) 5029.
[10] T. Van Buuren, et al., Phys. Rev. Lett. 80 (17) (1998) 3803.
[11] J. Fandiño, A. Ortiz, L. Rodríguez-Fernández, J.C. Alonso, J. Vac. Sci. Technol. A 22 (3) (2004) 570.
[12] M. Mayer, SIMNRA User's Guide, Version 4.4, Max Planck-Institute für Plasmaphysik, Garching, 1997.
[13] J. Aguilar-Hernández, et al., Jpn. J. Appl. Phys. Part I 33 (1994) 37.
[14] A.C. Adams, Solid State Technol. 26 (1–4) (1983) 135.
[15] J.C. Alonso, R. Vazquez, A. Ortiz, V. Pankov, E. Andrade, J. Vac. Sci. Technol. A 16 (1998) 3211.
[16] G. Santana, J. Fandiño, A. Ortiz, J.C. Alonso, J. Non-Cryst. Solids 351 (2005) 922.
[17] G. Santana, et al., Appl. Phys. Lett. 88 (2006) 041916.
[18] D.V. Tsu, G. Lucovsky, J. Vac. Sci. Technol. A 480 (1986).
[19] V. Baek-Hyun Kim, et al., Appl. Phys. Lett. 86 (2005) 091908.
[20] L. Pavesi, et al., Nature 408 (2000) 440.
[21] P.M. Fauchet, Materials Today, vol. 26, January 2005.
[22] Tae-Youb Kim, et al., Appl. Phys. Lett. 85 (2004) 5355.
[23] H. Shirai, Y. Fujimura, S. Jung, Thin Solid Films 407 (2002) 12.
[24] B.M. Monroy, et al., Photoluminescence of as-grown silicon nanocrystals embedded in silicon nitride: influence of atomic hydrogen abundance. J. Nanosci. Nanotechnol. (2008).